

Current density distribution for the quantum Hall effect

Serkan Sirt¹ and Stefan Ludwig^{1,*}

¹Paul-Drude-Institut für Festkörperelektronik, Leibniz-Institut im Forschungsverbund Berlin e.V., Hausvogteiplatz 5-7, 10117 Berlin, Germany

Our microscopic understanding of the integer quantum Hall effect is still incomplete. For decades, there has been a controversial discussion about “where the current flows” if the Hall resistance is quantized. Here, we qualitatively analyze the current density distribution in a Hall bar based on the screening properties of a two-dimensional electron system in the quantum Hall regime. Beyond previous publications, we include a closed loop persistent current that exists inside a Hall bar if the Hall resistance is quantized. We find, that the persistent current density decreases with increasing Hall voltage. Accounting for this dependence, we find, that the current flows in the opposite directions along opposite edges of the Hall bar, while the imposed current flows unidirectionally and only on the side of the Hall bar connected with its higher electrical potential edge.

I. INTRODUCTION

The integer quantum Hall effect (QHE) is one of the most fundamental and important phenomena in condensed matter physics. The quantized Hall resistance serves as a reference for the SI (Système International) unit system [1, 2], while new applications based on the QHE are likely to emerge in the context of quantum technologies. To realize such applications, it is important to understand the microscopic distributions of the electrostatic potential as well as the current density. For instance, the electrostatic details influence the stability of the quantized Hall plateaus, while the current density distribution also affects the quantum mechanical phase of the charge carriers [3]. For a known confinement potential of a hypothetical Hall bar without disorder, the distribution of the electrostatic potential can be numerically predicted with a high accuracy [4]. Nevertheless, the question of how to infer from the electrostatics to the microscopic distribution of the current in the case of the QHE is still the subject of controversial debate. Clarity will not only pave the way for new applications but also enhance our understanding of the fractional, spin or anomalous quantum Hall effects.

The text book explanation of the QHE, namely the Landauer-Büttiker picture, suggests that for the plateaus of the QHE all current flows inside one-dimensional channels along the edges of the Hall bar [5, 6]. This view is challenged by experiments [7–10] and theoretical calculations taking into account the Coulomb screening of the charge carriers [4, 11, 12]. Both show, that for specific regions of the plateaus the Hall voltage drops continuously across the Hall bar. Since current is generated by electric fields, this indicates the existence of bulk currents flowing far away from the edges of the Hall bar. Recently, such bulk currents have been directly measured in a narrow, high mobility Hall bar [13]. Recent multiterminal experiments probing the distribution of I_{impo} into various grounded contacts, however, suggest that for the entire plateaus I_{impo} follows a chiral trajectory, i.e., along the sample edge from contact to contact, while in between plateaus, I_{impo} is unidirectional as described by the Drude model [14].

In the present article, we present a qualitative model for the current density distribution, which explains all these findings.

We restrict our analysis to the plateaus of the QHE within the scope of the screening theory of the QHE [4, 11, 12, 15–18]. Our analysis builds on the calculations of the screening theory for the electrostatic potential distribution similar as in a previous prediction of the current density distribution [19], but we include a closed loop persistent current, I_{pers} , that was completely neglected in Ref. [19]. The persistent current is confined inside the Hall bar and exists in addition to the current, I_{impo} , imposed on the Hall bar through ohmic contacts, if the Hall resistance is quantized. I_{pers} directly depends on I_{impo} , which affects the distribution of the overall current, $I_{\text{impo}} + I_{\text{pers}}$, inside the Hall bar. Taking this dependence into account, we find, that the current flow is chiral, in the sense that the current flows in opposite directions along the opposite edges of a Hall bar. Subtracting the persistent current density from the overall current yield the imposed current. We find, that the imposed current flows unidirectionally and is concentrated on the side of the Hall bar with the higher electrical potential. It vanishes along the edge with the lower electrical potential. This result contradicts Ref. [19], which predicted that the imposed current flows unidirectionally on *both* sides of the Hall bar.

Non-local nature of the QHE and persistent current

The ballistic trajectory of a charged particle exposed to a magnetic field is chiral, a fundamental property related with the axial symmetry of the magnetic field vector. In solids, however, boundary conditions and momentum scattering can alter the impact of the axial symmetry and obscure the chirality of trajectories. This is clearly the case for the classical Hall effect described by the Drude model, which predicts a homogeneous unidirectional current density. The Drude model uses a relaxation time ansatz, which is local in nature and justified in the diffusive regime for $\mu B \lesssim 1$, where μ is the mobility [14].

The situation is different in the regime of the QHE with $\mu B \gg 1$ (and low enough temperature), where the current density is governed by the Landau quantization [20]. In the two-dimensional electron system (2DES) of a Hall bar and for the plateaus of a quantized Hall resistance, it gives rise to regions in which a local energy gap suppresses carrier scattering and Coulomb screening. In such regions, the sloped

* ludwig@pdi-berlin.de

electrostatic potential caused by the lateral confinement of the Hall bar, provides the driving force of a dissipationless persistent current. It flows along a chiral loop along the sample edge even inside an unbiased Hall bar [16]. Applying a voltage between ohmic contacts of the Hall bar, breaks the equilibrium by imposing an external current, I_{impo} . The latter generates the Hall voltage, $V_H = R_H I_{\text{impo}}$, dropping between the sample edges, where $R_H = h/(e^2 v)$ is the Hall resistance with filling factor v , elementary charge e and Planck constant h . Throughout quantized plateaus of the integer QHE, the filling factor remains integer within the extended regions of suppressed Coulomb screening and, I_{impo} , too, flows dissipationless through the Hall bar. The dissipation implied by the Hall resistance happens within “hot-spots” near the current carrying contacts [21, 22]. Both, “hot-spots” and persistent current are signatures of a non-local nature of the QHE. The current density distribution is strongly affected by this non-locality including a cross dependence $I_{\text{pers}}(I_{\text{impo}})$. This means in particular, that in order to determine the distribution of I_{impo} , it is necessary to consider the complete current density, $j = j_{\text{impo}} + j_{\text{pers}}$.

II. SCREENING THEORY

Exposing a 2DES to a high perpendicular magnetic field leads to the collapse of the density of states (DOS) into discrete LLs, the physical cause of the QHE. The Landauer-Büttiker picture of the QHE [5, 6], neglects the Coulomb interaction between charge carriers. However, the energy gap between LLs would then lead to displacements of the electrons causing high local charges [15]. The screening theory fixes this problem by taking into account the direct Coulomb interaction between carriers [4, 11, 12, 15–18]. This way, it accounts for the tendency of the carriers to minimize the free energy by redistribution (thereby avoiding high local charges) [15]. Nevertheless, in some regions of the 2DES, all LLs still end up to be either completely filled or empty, such that a local energy gap,

$$\Delta E = \begin{cases} g\mu_B B & ; \text{for odd } v \\ \hbar\omega_c - g\mu_B B & ; \text{for even } v \end{cases}, \quad (1)$$

remains, where g is the Landee g-factor, μ_B the Bohr magneton, v the filling factor and ω_c the cyclotron frequency. For $k_B T \ll \Delta E$ and low enough disorder, this gap locally suppresses scattering of electrons because of a lack of accessible unoccupied states. In a sense, the electrons behave like an incompressible liquid in these regions, which are therefore called incompressible strips (ICSs). The screening theory proposes a fragmentation of the Hall bar in compressible perfectly screened regions, separated by the unscreened ICSs [4, 11, 12]. Inside a compressible region, one partly filled LL is pinned to the locally constant chemical potential $\mu(y)$, hence the energies of all LLs, ε_v , are constant. Consequently, inside the unscreened ICSs, $\mu(y)$ and $\varepsilon_v(y)$ vary by the amount of the energy gap.

In Fig. 1, we sketch a typical situation as it is predicted by the screening theory near the low magnetic field end of

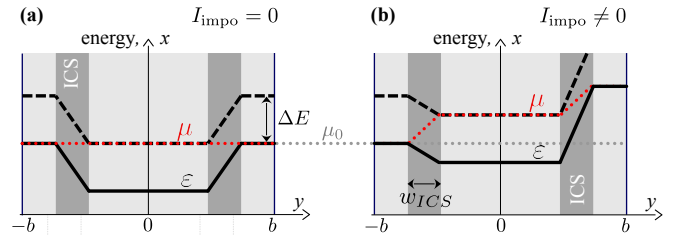


Figure 1. Qualitative sketches of the predictions of the screening theory for the first plateau ($v = 1$) of the QHE featuring the case of two ICSs near the edges of the Hall bar at $y = \mp b$. In (a), we assume $I_{\text{impo}} = 0$, such that $\mu = \mu_0$ is constant. In (b), we illustrate the effect of $I_{\text{impo}} \neq 0$ in the linear approximation, cf. main text. Energy $\varepsilon(y)$ of the first LL (solid line), the second LL (dashed line), and the chemical potential $\mu(y)$ (dotted red line). Only inside the ICSs (dark gray background) $d\varepsilon/dy \neq 0$ and $d\mu/dy \neq 0$.

the first plateau of the QHE, i.e., for $v = 1$ inside the ICSs (assuming a symmetric confinement potential). In Fig. 1(a) we depict the equilibrium situation for $I_{\text{impo}} = 0$ and $\mu_0 = \text{const}$, while in Fig. 1(b) we show a linear approximation for $I_{\text{impo}} \neq 0$ and varying $\mu_0(y)$. The energies, $\mu_0(y)$ and $\varepsilon(y) \equiv \varepsilon_1(y)$ vary only within the ICSs. However, their actual values depend on I_{impo} even inside the compressible region between the ICSs.

The early formulations of the screening theory were content with analytical and first self-consistent approximations [15] of the distribution of the electron density based on the Poisson equation and using the Thomas-Fermi approximation [16]. Later, the idea was refined by applying a self-consistent non-linear Hartree-type calculation and accounting for the quantum mechanical wave properties of the electrons by means of a Gaussian broadening of the LLs [11, 12]. Recently, (for high magnetic fields) the electrostatic results were confirmed for low integer filling factors within a full self-consistent approach of the quantum-electrostatic problem without using the Thomas-Fermi approximation [23].

Electrostatics of the QHE

We consider a Hall bar with edges at $y = \pm b$, defined for the carrier density $n_s > 0$ for $-b < y < b$, see Fig. 1. A current, I_{impo} , can be imposed between source (S) and drain (D) contacts, ideally positioned far away (at $x = \mp\infty$) along the vertical axis in the sketches in Fig. 1. In our sketches, we show a typical case as it occurs for a quantized Hall resistance near the low magnetic field end of the plateau. The local filling factor inside the ICSs is $v(y) = 1$. If the current flows inside the ICSs, it is carried by a single (spin polarized) LL with energy $\varepsilon(y)$. The energy of the second LL is higher by the Zeeman splitting $\Delta E = g\mu_B B$. As sketched in Fig. 1, there exist compressible strips between the edges and the ICSs, where the first LL is pinned to the chemical potential ($v < 1$) and a compressible bulk region between the ICSs, where the second LL is pinned to the chemical potential and partly occupied ($1 < v < 2$). For simplicity, we neglect many

body correlations, interference effects or details at the interface between compressible regions and the ICSs. Further, we consider I_{impo} to be small compared to the break-down current [24], such that a quantized plateau and ICSs can exist, and assume an idealized 2DES at zero temperature without disorder and a symmetric confinement potential. Moderate disorder effects [25] as well as asymmetric confinement [26] would have quantitative consequences but will not affect the qualitative findings of this article.

Geometry of the ICSs – linear approximation

In Fig. 1, we assumed that the width, w_{ICS} , of the ICSs is independent of I_{impo} . This corresponds to the linear approximation of the screening theory for a symmetric Hall bar. A more accurate examination reveals a non-linear relation between the imposed current and the induced change of the electrostatic potential, which can be accounted for in a self-consistent numerical calculation [4]. Qualitatively, the non-linear dependence is already present in a simple electrostatic approximation considering the local energy balance. It considers the Coulomb energy, E_C , caused by charge separation across an ICS because of its constant carrier density. Requiring $E_C = \Delta E$, it predicts for the equilibrium $w_{\text{ICS}} \propto \sqrt{\Delta E}$ [15]. Applying the same argument for $I_{\text{impo}} \neq 0$ results (in the limit of individual edge ICSs) in $w_{\text{ICS}} \propto \sqrt{\Delta E + \Delta\mu}$, where $\Delta\mu$ is the change of $\mu(y)$ across an ICS. Because of the confinement, ΔE is negative on one and positive on the other side of the Hall bar, cf. Fig. 1(a), while the change of the chemical potential across an ICS, $\Delta\mu$, has the identical sign for all ICSs, see Fig. 1(b). Therefore, w_{ICS} is reduced on one and increased on the other side of the Hall bar. To keep our discussion simple, in Fig. 1 we stick to the linear approximation, which predicts constant w_{ICS} and corresponds to the first loop of the self-consistent iterations [4]. However, the actual increase of $\Delta E \propto B$ as B is increased along a plateau of the QHE leads to the formation of a bulk ICS towards the high magnetic field end of a plateau [12]. Since this bulk ICS explains the measured bulk current [13] and bulk variations of $\mu(y)$ on the plateaus [10], we consider this limit in the right hand column of Fig. 2. Note that, considering the non-linear screening behavior quantitatively would require self-consistent numerical calculations as in Ref. [12] but wouldn't change our qualitative arguments below.

III. CURRENT DENSITY DISTRIBUTION FOR THE QHE

Previous discussion of where the current flows

The current density distribution for the case of a quantized Hall resistance became the subject of controversial discussions [27, 28] shortly after the discovery of the QHE, which are still continuing. The common non-interacting Landauer-Büttiker picture assumes current flow within compressible one-dimensional edge channels [6]. Taking into account the

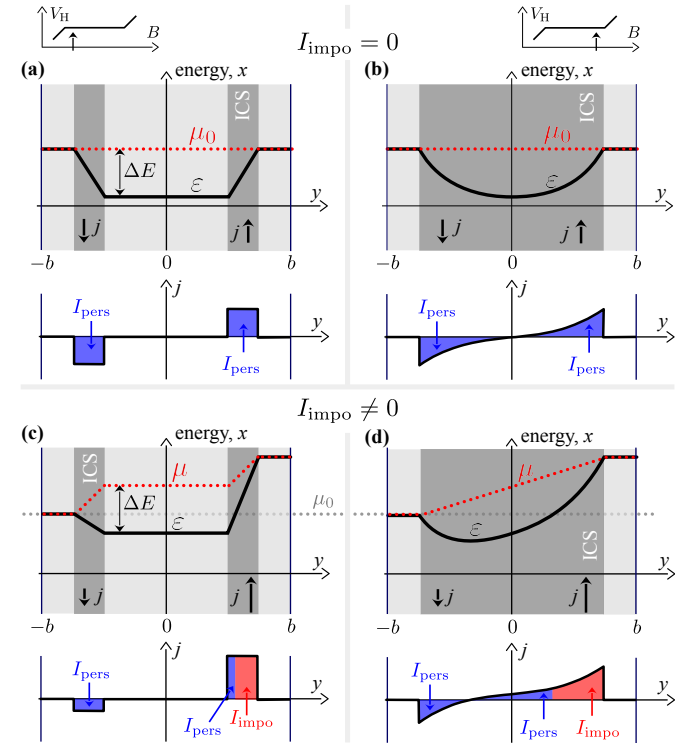


Figure 2. Extension of Fig. 1 featuring the current density for two different magnetic fields along the first plateau, as depicted in the insets at the upper end of the figure. Panels (a) and (c) on the left hand side illustrate the case of two separate ICSs, which occurs for B near the low magnetic field end of the first plateau. Panels (b) and (d) on the right show one single ICS extending through most of the bulk of the Hall bar, which occurs for B near the high magnetic field end of the first plateau. Shown are the energy $\varepsilon(y)$ of the first LL (solid line), the chemical potential $\mu(y)$ (red dotted line), the current density directions along $\pm x$ inside the ICSs (dark gray background) and, in the line plots the actual current densities $j(y)$ in arbitrary units. Negative currents (flowing in the $-x$ -direction) correspond to the integral $\int_{j<0} dy j$, positive currents to $\int_{j>0} dy j$. Regions with $\varepsilon < \mu_0$ contribute to I_{pers} , regions with $\varepsilon \geq \mu_0$ to I_{impo} . Finite I_{impo} causes I_{pers} to decrease.

Coulomb interaction of the carriers, Chklovskii et al. predicted the formation of ICSs [15] and then realized, calculating the ballistic current through a narrow gate defined channel, that for a quantized Hall resistance the current flows inside the ICSs [16]. Gerhardts and collaborators used a local version of Ohm's law assuming that the imposed current density, $j_{\text{impo}}(y)$, is proportional to the gradient of the chemical potential, $d\mu/dy$, which they calculated based on the screening theory [19]. Since $d\mu/dy = 0$ within compressible regions, they confirmed that the current flows inside the ICSs. However, by assuming $j_{\text{impo}} \propto |d\mu/dy|$ in their calculations, they completely neglected the persistent current density, j_{pers} , which led them to the prediction that the imposed current flows unidirectionally through all existing ICSs, i.e., in the same direction on both sides of the Hall bar [19]. Another approach predicting j_{impo} uses the continuity equation and finds $j_{\text{impo}} \neq 0$ inside compressible regions [23]. We find this approach ques-

tionable, mainly because it is restricted to $I_{\text{impo}} \sim 0$ (linear response) and, hence, fails to account for the non-linear nature of the QHE, which matters for reasonable values of V_H .

Model for the current density

In the present article, we acknowledge in agreement with Refs. [4, 16, 19, 29] that the current flows inside the ICSs. However, instead of focusing on the gradient of the chemical potential, which was used in Ref. [19] to predict j_{impo} , we go back to the original approach by Chklovskii et al. [16] and consider the complete current density $j = j_{\text{impo}} + j_{\text{pers}}$, which is carried by the fully occupied LLs inside the ICSs. We emphasize, that inside the unscreened ICSs the electrons of a LL are driven by the local electric field, which is identical to the gradient of the LL energy, $\vec{E} = -\vec{\nabla}\varepsilon/e$ and differs from the gradient of the chemical potential.

The current density carried by an individual LL in the absence of scattering, i.e., inside an ICS, follows from fundamental relations: it is given by $\vec{j}_{\text{LL}} = -e n_{\text{LL}} \vec{v}$ with the velocity $\vec{v} = \vec{E} \times \vec{B}/B^2$ of an electron and the carrier density $n_{\text{LL}} = Be/h = n_s/v$ of the LL. Inside an ICSs the local filling factor, v , is a constant integer. For our Hall bar geometry we have $\vec{E} = -\frac{1}{e} \frac{d}{dy} (0, \varepsilon, 0)^T$, such that for $\vec{B} = (0, 0, B)^T$ inside an ICS a current with density $\vec{j} = (j, 0, 0)^T$ flows in the x -direction with

$$j = v j_{\text{LL}} = \pm v \frac{e}{h} \frac{d\varepsilon}{dy}. \quad (2)$$

For all practical cases, the confinement potential of the Hall bar has opposite slopes along its two edges, cf. Fig. 2. Therefore, \vec{E} points in opposite directions and j is positive on one side of the Hall bar and negative on its other side.

In Fig. 2, we qualitatively sketch our prediction for $v = 1$ based on Eq. (2) and the screening theory [12]. The four panels show for four different characteristic situations $\varepsilon(y) \equiv \varepsilon_1(y)$ (solid lines), $\mu(y)$ (dotted red lines) and the related $j(y)$ (lower panels) across a Hall bar. ICSs are indicated by a dark gray background, compressible regions by light gray. Only within the unscreened ICSs the LL energy, $\varepsilon(y)$, varies and $j \neq 0$. In Figs. 2a and 2b, we consider the equilibrium with $I_{\text{impo}} = 0$, while in Figs. 2c and 2d we added a finite $I_{\text{impo}} \neq 0$. In Figs. 2a and 2c, we depict the case of two ICSs near the edges of the Hall bar, while in Figs. 2b and 2d, we sketch the case of a single bulk ICS. The screening theory predicts these two cases to occur at the two ends of the plateau of a quantized Hall resistance as indicated in the insets above Figs. 2a and 2b [12].

Because, the persistent current flows in a closed loop, its density fulfills $\int_{-b}^b dy j_{\text{pers}} = 0$. Hence, we can define I_{pers} by dividing this integral into two regions: $I_{\text{pers}} \equiv -\int_{-b}^{y(j=0)} dy j_{\text{pers}} = \int_{y(j=0)}^b dy j_{\text{pers}}$, which has the identical absolute value on both sides of the Hall bar. In contrast to I_{pers} , the imposed current enters the Hall bar and leaves it through the source and drain contacts. Therefore, I_{impo} corresponds to

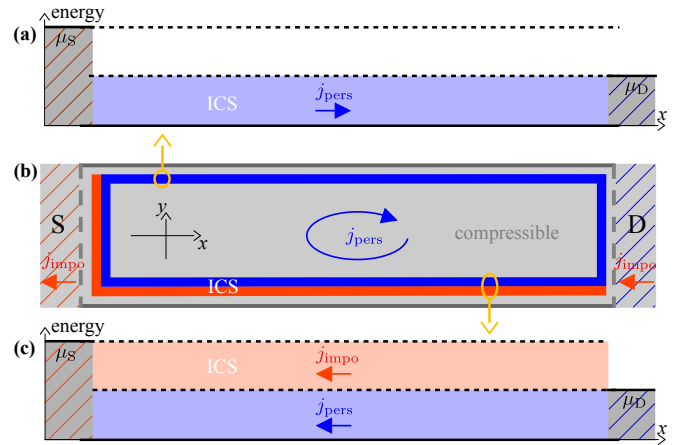


Figure 3. Illustration of geometry in (b) of the ICS corresponding to the non-equilibrium situation with $I_{\text{impo}} \neq 0$ of Fig. 2(b); (a) and (c) are energy diagrams of the ICS along the upper and lower edges, respectively. States contributing to j_{pers} are indicated in blue and those of j_{impo} in red. The persistent current describes a closed path inside the Hall bar as all contributing states have energies below the chemical potentials of both leads, $E < \mu_S, \mu_D$. The imposed current is carried by states with energies $\mu_S \geq E > \mu_D$. Its electrons enter the Hall bar from the source contact, move along its high potential (lower) edge and leave it into empty states of the drain contact.

the integral of the complete current density over the full width of the Hall bar, $I_{\text{impo}} = \int_{-b}^b dy j = \int_{-b}^b dy j_{\text{impo}}$.

I_{impo} generates the Hall voltage between the two edges, $|V_H| = |\mu(b) - \mu(-b)|/e = h/e^2/I_{\text{impo}}$ (for $v = 1$), cf. Figs. 2c and 2d. In our sketches we chose the chemical potential at the drain contact as reference, $\mu(-b) = \mu_0$. In equilibrium, i.e., for $I_{\text{impo}} = 0$, the chemical potential is constant, $\mu(y) = \mu_0$. For $I_{\text{impo}} \neq 0$, $\mu(y) \geq \mu_0$ increases monotonously between the edges, while it always remains constant within the compressible regions. An increase of $\mu(y)$ corresponds to an accumulation of a negative charge. Therefore, $\varepsilon(y)$ increases accordingly (compare the upper panels for $I_{\text{impo}} = 0$ with the lower panels for $I_{\text{impo}} \neq 0$ in Fig. 2). Importantly, the increase of $\varepsilon(y)$ yields a decrease of j for $-b < y \lesssim 0$ (the low potential side of the Hall bar) and an increase of j for $0 \lesssim y < b$ (the high potential side). Because $\int_{-b}^b dy j_{\text{pers}} = 0$, the decrease of j on the low potential side corresponds to a decrease of I_{pers} . The increase of j on the high potential side then points to a combination of the established decrease of I_{pers} together with I_{impo} flowing there.

Within our linear approximation, see Sec. II, for $eV_H \ll 2\Delta E$ we find an opposite direction of the current flow on the two sides of the Hall bar, i.e., a chiral current flow. The case $eV_H \sim 2\Delta E$, which is clearly beyond the scope of our approximation, would result in a break down of the ICSs. However, as long as an ICS exists on the low potential side, we expect $d\varepsilon/dy$ to remain ≤ 0 there, supported by numerical calculations [24]. We conclude: whenever the Hall resistance is quantized (ICSSs exist), the current flow is chiral.

The illustration in Fig. 3, offers an alternative point of view for the case of two ICSs in the vicinity of the edges. In panel

(b), we sketch a minimalistic model of a Hall bar. It consists of two edges connecting the source (S) and drain (D) contacts fixed to the chemical potentials $\mu_S > \mu_D$. The persistent current flows in a closed loop inside the ICS (blue). The imposed current flows through the ICS from drain to source (red). The corresponding electrons moving from source to drain pin the chemical potential of the lower edge to μ_S . Since j_{impo} flows entirely along the lower edge of the Hall bar, its upper edge remains at μ_D . Figures 3 (a) and (c) illustrate the chemical potentials of the contacts and the energy range of the current carrying (occupied) states inside the ICS along the upper versus lower edge, respectively. Shaded regions indicate occupied states (at $T = 0$), gray inside the contacts, blue inside the ICS at energies $E < \mu_D$, and red inside the ICS at energies $\mu_D < E \leq \mu_S$. Electrons with $E \leq \mu_D$ (blue) contribute to j_{pers} , electrons with $E > \mu_D$ (red) contribute to j_{impo} . Clearly, j_{pers} follows a closed path inside the Hall bar as for $E \leq \mu_D$ no unoccupied states are available in the leads. In contrast j_{impo} is carried by electrons emitted from the source contact, which then leave the Hall bar into the drain contact, cf. Fig. 3(c). Reflecting the chiral nature of the ICSs, predefined by the local gradients of the LL energies, cf. Fig. 2(b), j_{impo} flows entirely inside the ICS along the high potential (lower) edge.

IV. SUMMARY

In summary, by applying the screening theory and considering the complete current density $j = j_{\text{impo}} + j_{\text{pers}}$ inside the

Hall bar, we find that for a quantized Hall resistance

- (i) the current flows inside ICSs,
- (ii) the current flow is chiral,
- (iii) the current density consist of a persistent and an imposed contribution, $j = j_{\text{pers}} + j_{\text{impo}}$,
- (iv) I_{pers} is maximal for $I_{\text{impo}} = 0$ and decreases as $|I_{\text{impo}}|$ is increased,
- (v) I_{impo} flows entirely on the high potential side of the Hall bar.

Finally, we note that the occurrence of bulk current is not in conflict with chiral current flow as long as scattering of the carriers is suppressed inside the bulk ICS, cf. Fig. 2.

ACKNOWLEDGEMENT

This work was funded by the Deutsche Forschungsgemeinschaft (DFG, German Research Foundation) – 218453298.

CONTRIBUTIONS OF THE AUTHORS

S. L. wrote the article. S. S. contributed in many fruitful discussions and carefully read the article.

REFERENCES

- [1] BIPM, *Le Système international d'unités / The International System of Units ('The SI Brochure')*, ninth ed. (Bureau international des poids et mesures, 2019).
- [2] F. Delahaye and B. Jeckelmann, Revised technical guidelines for reliable dc measurements of the quantized Hall resistance, *Metrologia* **40**, 217 (2003).
- [3] N. Ofek, A. Bid, M. Heiblum, A. Stern, V. Umansky, and D. Mahalu, Role of interactions in an electronic fabry-perot interferometer operating in the quantum hall effect regime, *Proceedings of the National Academy of Sciences* **107**, 5276 (2010), <https://www.pnas.org/doi/pdf/10.1073/pnas.0912624107>.
- [4] R. R. Gerhardts, The effect of screening on current distribution and conductance quantisation in narrow quantum Hall systems, *physica status solidi (b)* **245**, 378 (2008).
- [5] M. Büttiker, Four-terminal phase-coherent conductance, *Phys. Rev. Lett.* **57**, 1761 (1986).
- [6] M. Büttiker, Absence of backscattering in the quantum Hall effect in multiprobe conductors, *Phys. Rev. B* **38**, 9375 (1988).
- [7] P. F. Fontein, J. A. Kleinen, P. Hendriks, F. A. P. Blom, J. H. Wolter, H. G. M. Lochs, F. A. J. M. Driessens, L. J. Giling, and C. W. J. Beenakker, Spatial potential distribution in GaAs/Al_xGa_{1-x}As heterostructures under quantum hall conditions studied with the linear electro-optic effect, *Phys. Rev. B* **43**, 12090 (1991).
- [8] A. Yacoby, H. Hess, T. Fulton, L. Pfeiffer, and K. West, Electrical imaging of the quantum hall state, *Solid State Communications* **111**, 1 (1999).
- [9] K. L. McCormick, M. T. Woodside, M. Huang, M. Wu, P. L. McEuen, C. Duruoz, and J. S. Harris, Scanned potential microscopy of edge and bulk currents in the quantum Hall regime, *Phys. Rev. B* **59**, 4654 (1999).
- [10] P. Weitz, E. Ahlsweide, J. Weis, K. Klitzing, and K. Eberl, Hall-potential investigations under quantum Hall conditions using scanning force microscopy, *Physica E: Low-dimensional Systems and Nanostructures* **6**, 247 (2000).
- [11] A. Siddiki and R. R. Gerhardts, Thomas-fermi-poisson theory of screening for laterally confined and unconfined two-dimensional electron systems in strong magnetic fields, *Phys. Rev. B* **68**, 125315 (2003).
- [12] A. Siddiki and R. R. Gerhardts, Incompressible strips in dissipative Hall bars as origin of quantized Hall plateaus, *Phys. Rev. B* **70**, 195335 (2004).
- [13] S. Sirt, V. Y. Umansky, A. Siddiki, and S. Ludwig, Transition from edge- to bulk-currents in the quantum hall regime, *Applied Physics Letters* **126**, 243101 (2025).
- [14] S. Sirt, M. Kamm, V. Y. Umansky, and S. Ludwig, Chiral nature of current flow in the regime of the quantized hall effect (2024), [arXiv:2407.01277 \[cond-mat.mes-hall\]](https://arxiv.org/abs/2407.01277).
- [15] D. B. Chklovskii, B. I. Shklovskii, and L. I. Glazman, Electrostatics of edge channels, *Phys. Rev. B* **46**, 4026 (1992).

- [16] D. B. Chklovskii, K. A. Matveev, and B. I. Shklovskii, Ballistic conductance of interacting electrons in the quantum Hall regime, *Phys. Rev. B* **47**, 12605 (1993).
- [17] M. M. Fogler and B. I. Shklovskii, Resistance of a long wire in the quantum Hall regime, *Phys. Rev. B* **50**, 1656 (1994).
- [18] K. Lier and R. R. Gerhardts, Self-consistent calculations of edge channels in laterally confined two-dimensional electron systems, *Phys. Rev. B* **50**, 7757 (1994).
- [19] K. Güven and R. R. Gerhardts, Self-consistent local equilibrium model for density profile and distribution of dissipative currents in a hall bar under strong magnetic fields, *Phys. Rev. B* **67**, 115327 (2003).
- [20] K. von Klitzing, G. Dorda, and M. Pepper, New method for high-accuracy determination of the fine-structure constant based on quantized Hall resistance, *Phys. Rev. Lett.* **45**, 494 (1980).
- [21] U. Klaß, W. Dietsche, K. von Klitzing, and K. Ploog, Imaging of the dissipation in quantum-hall-effect experiments, *Zeitschrift für Physik B Condensed Matter* **82**, 351 (1991).
- [22] S. Komiyama, H. Sakuma, K. Ikushima, and K. Hirakawa, Electron temperature of hot spots in quantum hall conductors, *Phys. Rev. B* **73**, 045333 (2006).
- [23] P. Armagnat and X. Waintal, Reconciling edge states with compressible stripes in a ballistic mesoscopic conductor, *Journal of Physics: Materials* **3**, 02LT01 (2020).
- [24] K. Panos, R. R. Gerhardts, J. Weis, and K. von Klitzing, Current distribution and hall potential landscape towards breakdown of the quantum hall effect: a scanning force microscopy investigation, *New Journal of Physics* **16**, 113071 (2014).
- [25] A. Siddiki and R. R. Gerhardts, Range-dependent disorder effects on the plateau-widths calculated within the screening theory of the iqhe, *International Journal of Modern Physics B* **21**, 1362 (2007).
- [26] A. Siddiki, J. Horas, D. Kupidura, W. Wegscheider, and S. Ludwig, Asymmetric nonlinear response of the quantized hall effect, *New Journal of Physics* **12**, 113011 (2010).
- [27] R. B. Laughlin, Quantized hall conductivity in two dimensions, *Phys. Rev. B* **23**, 5632 (1981).
- [28] B. I. Halperin, Quantized hall conductance, current-carrying edge states, and the existence of extended states in a two-dimensional disordered potential, *Phys. Rev. B* **25**, 2185 (1982).
- [29] R. R. Gerhardts, Self-consistent theory of screening and transport in narrow, translation-invariant Hall bars under the conditions of the integer quantum-Hall-effect, *Recent Progress in Materials* **02**, 007 (2020).